Study of nonproportionality in the light yield of inorganic scintillators

Singh, Jai

Published in:
Journal of Applied Physics

DOI:
10.1063/1.3607247

Published: 15/07/2011

Document Version
Publisher's PDF, also known as Version of record

Study of nonproportionality in the light yield of inorganic scintillators

Jai Singh[a)]
School of Engineering and IT, B-purple-12, Faculty of EHSE, Charles Darwin University, Darwin, Northern Territory 0909, Australia

(Received 24 January 2011; accepted 31 May 2011; published online 20 July 2011)

Using a phenomenological approach, the light yield is derived for inorganic scintillators as a function of the rates of linear, bimolecular, and Auger processes occurring in the electron track initiated by an x ray or a γ-ray photon. A relation between the track length and incident energy is also derived. It is found that the nonproportionality in the light yield can be eliminated if either nonlinear processes of interaction among the excited electrons, holes, and excitons can be eliminated from occurring or the high density situation can be relieved by diffusion of carriers from the track at a faster rate than the rate of activation of nonlinear processes. The influence of the track length and radius on the yield nonproportionality is discussed in view of the known experimental results. Inventing new inorganic scintillating materials with high carrier mobility can lead to a class of proportional inorganic scintillators. Results agree qualitatively with experimental results for the dependence of light yield on the incident energy. © *2011 American Institute of Physics*. [doi:10.1063/1.3607247]

I. INTRODUCTION

Scintillators are used as radiation detectors in nuclear medical imaging systems, like single photon emission computed tomography (SPECT) and positron emission tomography (PET), which are expected to be the most popular future diagnostic systems for human health in the world.[1] This is due to the fact that these systems have faster patient throughput, greater patient comfort, diagnostic certainty, and staging accuracy, which enable practitioners better treatment planning of diseases like cancers, tumors, heart diseases, and Alzheimer's. In addition, there are more than 49 000 airports and 926 seaports at present in the world which require detectors of contraband nuclear materials at each of their entrances for their country's border and homeland security. Each of these detecting systems also requires, now more than ever, scintillators as detectors. Most existing scintillators suffer from poor energy resolution, which limits the accuracy of their imaging capacity. Therefore, it is very timely and desirable to either invent new scintillators which have superior energy resolution or improve the energy resolution of existing ones or both. To achieve this, one has to understand very clearly why the existing scintillators have poor energy resolution and how to improve it.

A γ photon absorbed in a scintillator first creates a very high energy electron, which ionizes the medium of its track, and high density excited electron (e) and hole (h) pairs are generated through this ionization in a cascade process, eventually, with energies close to the bandgap; some of them recombine radiatively and some non-radiatively. The photons emitted due to the radiative recombination contribute to the light yield of a scintillator and are defined as the integrated light output per MeV of energy deposited in a scintillator. The light yield is not found to be constant with the incident γ energy, typically in the range of 10 keV to 1 MeV, in most scintillators, which is referred to as nonproportionality,[2,3] and it seriously affects their attainable energy resolution,[4] leading to poor quality and inaccurate imaging. Only a few attempts have been made, in theory,[5–7] to understand the problem of nonproportionality in inorganic scintillators. These studies reveal that higher order nonlinear quenching processes contribute to the nonproportionality. It is also established that, contrary to scintillators, in the similar γ-ray energy range, semiconductor detectors are almost perfectly proportional.[2] This raises the obvious question: why? If it is due to the nonlinear processes occurring within the electron track initiated by a γ-photon under the condition of high excitation density, then the nonproportionality should be observed in both scintillators as well as semiconductor detectors. For understanding this puzzle, two competing processes need to be considered in the track of an electron initiated by an incident γ-photon: the rate of creation of high density excitation in the track and that of depletion of these excited electron and hole pairs (e-h) from the track.[8,9] The second and third order (Auger type) processes become significant only when a created high density stays in the track longer than the decay time of these nonlinear processes. If all excited e-h pairs and excitons move away from the track faster than the decay time of nonlinear processes, then the contribution of nonlinearity to the light yield will be eliminated. That means the magnitude of mobility of charge carriers plays a very significant role in the nonproportional response of a scintillator. If electron and hole mobilities are significantly high in a material used as detector, the track will not get densely crowded with e-h excitations to activate the nonlinear processes.

In Table I, electron and hole mobilities are listed for a few semiconductor detectors and scintillators. The mobility data for scintillators are scarce in the literature. However, one can get some idea about the mobility from the effective mass of charge carriers in the valence and conduction bands, as the mobility is inversely proportional to the effective mass ($\mu_i = e\tau_i/m_i^*$, $i = e$ or h). Setyawan *et al.*[23] have recently performed very extensive calculations of the band structures

[a)]Electronic mail: jai.singh@cdu.edu.au.

TABLE I. List of the measured carrier mobility (cm^2/Vs) in some semiconductors and scintillators.

Semiconductors								
	Si	Ge	CZT	HgI_2	PbI_2	CdTe	InSb	GaAs
μ_e	1400[11]	3900[13]	1120[15]	67[16]	8[18]	945[15]	78000[19]	8800[19]
μ_h	450[12]	1900[14]	66[15]	4[17]	2[18]	66[15]	750[19]	400[19]
Scintillators								
	CsI	NaI	CaF_2(Eu)	BaF_2	GSO	NaCl		
μ_e	8±2[10]	0.11 (at 700 °C)[20]10[21]				1200 (7K)[22]		
μ_h								

and effective masses of charge carriers in most materials currently used as scintillators. In most scintillators considered in Ref. 23, except yttrium aluminium perovskite (YAP), the hole effective mass is heavier than the electron effective mass, and the ratio of hole effective mass to electron effective mass varies from 1.6 to 22. In YAP, this ratio is 0.83. It is also found in Ref. 23 that scintillators with this ratio close to unity are more proportional in their light yield. According to the effective mass theory, a heavier effective mass means greater localization and, hence, a charge carrier with larger effective mass is more localized than that with lighter effective mass.[24] In other words, a heavier effective mass particle will move slower than the lighter one. Furthermore, those scintillators in which a charge carrier has larger effective mass will consequently have lower mobility, and if created within the track of a γ-ray, it will not be able to clear the track as fast as in materials where the charge carrier has a lighter effective mass. If e-h pairs created in the track could not leave the track fast enough, the nonlinear processes of interaction will be activated, leading to nonradiative recombination within the track and, hence, causing nonproportionality in the scintillator's yield.

The purpose of this paper is to analyze the nonproportionality in scintillators as a function of linear and nonlinear radiative and nonradiative processes and to develop procedures of reducing/eliminating it. The approach followed here is initially phenomenological and similar to the recent work[6] with further developments along the approach followed in Ref. 5.

II. THEORY OF SCINTILLATOR LIGHT YIELD

Following Ref. 6, we consider a cylindrical track of an average radius r in a scintillating crystal, and only excitons and excited pairs of electron and hole (e-h pairs) are generated in the track. Phonons are, of course, generated in relaxation of energetic carriers and self-trapping of excitons. The details of phenomenological equations are given in Ref. 6 and, hence, not repeated here.

A. Excitation density and track length

The local density of excitation along a linear cylindrical track at any point x, denoted by $n(x)$, is given by[6]

$$n(x) = \frac{\left(-\frac{\partial E}{\partial x}\right)}{\pi r^2 E_{eh}}, \tag{1}$$

where E is the total initial energy incident at any point x, πr^2 is the average area of cross section of the track, and E_{eh} is the average energy required to create an excitation in a scintillator, which is assumed here to be three times the bandgap energy (E_g): $E_{eh} = 3E_g$. The total excitation density $n(x)$ is the sum of exciton density ($n_{ex}(x)$) and e-h pair density ($n_{eh}(x)$), $n(x) = n_{ex}(x) + n_{eh}(x)$, such that $n_{ex}(x) = f_x n(x)$ and $n_{eh}(x) = (1 - f_x)n(x)$ and $f(x)$ $(0 < f(x) < 1)$ is the fractional concentration of excitons in the track. For determining the total excitation concentration, n, one has to integrate Eq. (1) over the track length to get[6]

$$n = \frac{1}{\pi r^2 E_{eh}}\left[\frac{1}{L}\int_0^L \left(-\frac{dE}{dx}\right)dx\right] = \frac{1}{\pi r^2 E_{eh}}\left[\frac{1}{L}\int_0^E \left(-\frac{dE}{dx}\right)\left(\frac{dx}{dE}\right)dE = \frac{1}{\pi r^2 E_{eh}}\left[\frac{E}{L}\right]\right]. \tag{2}$$

However, this expression of the excitation concentration n is not very useful because one needs to know the length of the track, L, which depends on the energy and, hence, it is not easy to know for any scintillator. Using the Bethe expression for the stopping power[25] and following Jaffe,[5] it is also approximately obtained as

$$n \approx \left[\frac{20e^4\kappa^2 N_e}{E_{eh} r^2}\right]E^{-1}, \tag{3}$$

where e is the electronic charge, $\kappa = (4\pi\varepsilon_0)^{-1} = 8.9877 \times 10^9$, and $N_e \approx 10^{30}\mathrm{m}^{-3}$ is the density of ground-state electrons in the track. The approximate expression of n in Eq. (3) can be used to approximate the track length as a function of energy by comparing it with Eq. (2), and one thus obtains

$$L \approx \frac{E^2}{20\pi e^4 \kappa^2 N_e}. \tag{4}$$

According to Eq. (4), the track length is proportional to the square of the total deposited energy E by a γ-photon in the track in a scintillator. The interesting point is that the track length derived in this way, within the average radius of cross section approximation, does not depend on its own radius.

B. Scintillator light yield

In the track, all the radiative channels contribute to the emission of photons, which are detected and, hence, the light

yield or scintillator yield is defined as the total emitted photons divided by the total excitations created in the track. Considering only the linear, bimolecular (second order), and Auger (third order) processes occurring within the track, the scintillator yield is obtained as[6]

$$Y = \frac{a_1 n + a_2 n^2}{a_3 n + a_4 n^2 + a_5 n^3}, \tag{5}$$

where

$$a_1 = R_{1x}A + R_{1eh}B, \tag{6a}$$

$$A = \frac{[\gamma_{ex} + (R_{1eh} + K_{1eh})f_x]}{(R_{1x}+K_{1x})(R_{1eh}+K_{1eh}) + \gamma_{ex}(R_{1x}+K_{1x}) + \gamma_{xe}(R_{1eh}+K_{1eh})}, \tag{6b}$$

$$B = \frac{[(1-f_x)(R_{1x}+K_{1x}) + \gamma_{xe}]}{(R_{1x}+K_{1x})(R_{1eh}+K_{1eh}) + \gamma_{ex}(R_{1x}+K_{1x}) + \gamma_{xe}(R_{1eh}+K_{1eh})}, \tag{6c}$$

$$a_2 = \frac{R_{2x}}{2\tau_x}A^2 + \frac{R_{2eh}}{2\tau_{eh}}B^2; \quad \tau_x^{-1} = R_{1x} + K_{1x} \text{ and } \tau_{eh}^{-1} = R_{1eh} + K_{1eh}, \tag{6d}$$

$$a_3 = (R_{1x} + K_{1x})A + (R_{1eh} + K_{1eh})B, \tag{6e}$$

$$a_4 = \frac{(R_{2x} + K_{2x})}{2\tau_x}A^2 + \frac{(R_{2eh} + K_{2eh})}{2\tau_{eh}}B^2, \tag{6f}$$

$$a_5 = \frac{K_{3x}}{3\tau_x^2}A^3 + \frac{K_{3eh}}{3\tau_{eh}^2}B^3. \tag{6g}$$

Here, R_{ix} and K_{ix} denote the rates of radiative and non-radiative (quenching) recombination of excitons, respectively, and $i = 1$ and 2 denote linear (1) and bimolecular (2) processes. R_{ieh} and K_{ieh} ($i = 1$ and 2) are the corresponding rates of recombination for an e-h pair, and K_{3x} and K_{3eh} are rates of non-radiative Auger recombination of excitons and e-h pairs, respectively. It is assumed here that Auger processes do not contribute to any radiative recombination. γ_{ex} and γ_{xe} are rates of converting an e-h pair into an exciton and vice versa, respectively.

Using Eq. (3), the yield in Eq. (5) can be expressed as a function of the incident energy as

$$Y = \frac{a_1 + a_2 Q E^{-1}}{a_3 + a_4 Q E^{-1} + a_5 Q^2 E^{-2}}, \tag{7}$$

where

$$Q = \frac{20 e^4 \kappa^2 N_e}{E_{eh} r^2}. \tag{8}$$

Dividing the numerator of the yield in Eq. (7) by $a_2 Q$ and denominator by $a_4 Q$, Y can be expressed in the following form:

$$Y = \frac{a_2}{a_4}\frac{(H_1^{-1} + E^{-1})}{(H_2^{-1} + E^{-1} + H_3 E^{-2})}, \tag{9}$$

where

$$H_1 = \frac{a_2 Q}{a_1}, \quad H_2 = \frac{a_4 Q}{a_3}, \quad H_3 = \frac{a_5 Q}{a_4}. \tag{10}$$

It is to be noted that Q has the dimensions of energy/m^3 and H_1, H_2, and H_3 have the dimensions of energy. Although the yield expression of Eq. (9) is quite convenient,[5] it can only be used for scintillators where a_2 and a_4 are non-zero. Therefore, for retaining generality, only the yield in Eq. (7) will be considered here onwards. Moreover, the yield in Eq. (9) does not reflect very clearly the non proportional behavior, whereas it is obvious from Eq. (7) that the yield will be constant (proportional) in those scintillators where $a_2 = a_4 = a_5 = 0$ resulting $Y = a_1/a_3$. According to Eq. (6), a_2, a_4, and a_5 depend on the rates of bimolecular and Auger radiative and non-radiative processes, and $a_1$and a_3 depend only on the rates of linear radiative and nonradiative processes. This means that, if nonlinear processes can be eliminated from occurring within a scintillator, its yield will be proportional. More will be discussed on this issue in Sec. IV.

Experimentally, the scintillator yield is calculated as a customary or convention relative to the yield at an energy $E = 662$ keV. This can be obtained by dividing the yield in Eq. (7) by its value at $E = 662$ keV, and thus the relative yield is obtained as

$$Y_R = \frac{(a_1 + a_2 Q E^{-1})(a_3 + a_4 Q(662 \text{ keV})^{-1} + a_5 Q^2 (662 \text{ keV})^{-2})}{(a_1 + a_2 Q(662 \text{ keV})^{-1})(a_3 + a_4 Q E^{-1} + a_5 Q^2 E^{-2})}. \tag{11}$$

Provided a_1 and a_3 are nonzero and $a_2 = a_4 = a_5 = 0$, the above relative yield becomes perfectly proportional, i.e., $Y_R = 1$ at all energies. The relative yield derived here can be calculated for any scintillators if the rates of linear, bimolecular, and Auger recombination processes are known. Unfortunately, this is not the case. The rates of linear radiative (R_1) and nonradiative (K_1) processes are known for some scintillators, but the rates of nonlinear processes are in scarcity. Williams *et al.*[9] have recently measured K_2 in a few alkali halide scintillators as a function of time and discussed the dynamics of excitations within a track as a function of the time scale.

III. RESULTS

The derived relative scintillator yield in Eq. (11) is used here to calculate the yields in four scintillators considered in Ref. 6 because the linear and nonlinear rates have already been known or estimated for these scintillators, namely, NaI:Tl, BaF_2, Gd_2SiO_5:(GSO:Ce), and $LaCl_3$:Ce. Two of these scintillators, BaF_2 and GSO:Ce, have also been studied

TABLE II. Rate constants and other parameters used to calculate the scintillation light yield versus particle energy curves for four materials. Values in bold type were determined from independent measurements. Values in normal type were constrained as constants common to all four materials, since they could only be roughly estimated. Values in italics are varied as fitting parameters among the four materials [6].

Rate constants	NaI:Tl	BaF_2	GSO:Ce	$LaCl_3$:Ce
R_{1x}	$\mathbf{4.7\times10^{6}\ s^{-1}}$	$\mathbf{1.6\times10^{9}\ s^{-1}}$	$\mathbf{3\times10^{7}\ s^{-1}}$	$\mathbf{3\times10^{7}\ s^{-1}}$
K_{1x}	$\mathbf{1.2\times10^{6}\ s^{-1}}$	$\mathbf{4\times10^{8}\ s^{-1}}$	$\mathbf{3\times10^{6}\ s^{-1}}$	$\mathbf{3\times10^{6}\ s^{-1}}$
R_{1eh}	**0**	**0**	**0**	**0**
K_{1eh}	$3\times10^{6}\ s^{-1}$	$3\times10^{6}\ s^{-1}$	$3\times10^{6}\ s^{-1}$	$3\times10^{6}\ s^{-1}$
R_{2eh}	$\mathbf{3\times10^{-11}\ cm^3/s}$	$3\times10^{-11}\ cm^3/s$	$3\times10^{-11}\ cm^3/s$	$3\times10^{-11}\ cm^3/s$
K_{2eh}	$3\times10^{-12}\ cm^3/s$	$3\times10^{-12}\ cm^3/s$	$3\times10^{-12}\ cm^3/s$	$3\times10^{-12}\ cm^3/s$
R_{2x}	**0**	**0**	**0**	**0**
K_{2x}	$2\times10^{-11}\ cm^3/s$	$2\times10^{-11}\ cm^3/s$	$2\times10^{-11}\ cm^3/s$	$2\times10^{-11}\ cm^3/s$
K_{3eh}	$1\times10^{-29}\ cm^6/s$	$1\times10^{-29}\ cm^6/s$	$1\times10^{-29}\ cm^6/s$	$1\times10^{-29}\ cm^6/s$
K_{3x}	$1\times10^{-29}\ cm^6/s$	$1\times10^{-29}\ cm^6/s$	$1\times10^{-29}\ cm^6/s$	$1\times10^{-29}\ cm^6/s$
$\gamma_{eh\text{-}x}$	0	0	0	0
$\gamma_{x\text{-}eh}$	0	0	0	0
r (track rad.)	*6 nm*	*2 nm*	*4 nm*	*4 nm*

by Jaffe and, hence, results can be compared with those obtained in Ref. 5 as well. In the above four scintillators, the linear radiative rate of e-h pairs, R_{1eh} and the bimolecular excitonic radiative rate, R_{2x}, are set to be zero.[6] The rates used in the calculation here are re–listed from Ref. 6 in Table II for convenience. According to our model presented here, the scintillators can be classified in three categories: excitonic, non-excitonic, and intermediate, which are considered separately below.

A. Excitonic scintillators

In this category of scintillators, $f_x = 1$, which means only excitons are created within the track, and BaF_2 and GSO:Ce are considered to be in this category in Ref. 6. For these two scintillators, $a_2 = 0$ and, according to Eq. (6), $a_3 = 1$ for all four considered above. Therefore, the yield in Eq. (7) reduces to the following form:

$$Y = \frac{a_1}{1 + a_4 Q E^{-1} + a_5 Q^2 E^{-2}}, \tag{12}$$

and then the relative yield simplifies to

$$Y_R = \frac{1 + a_4 Q(662\ \text{keV})^{-1} + a_5 Q^2 (662\ \text{keV})^{-2}}{1 + a_4 Q E^{-1} + a_5 Q^2 E^{-2}}. \tag{13}$$

According to Eq. (13), a_1 does not contribute to the relative yield of excitonic scintillators, but it should be non-zero, and because $a_2 = 0$, the nonproportionality is caused only by the rate coefficients a_4 and a_5, which are obtained from Eq. (6) as

$$a_4 = \frac{(R_{2x} + K_{2x})}{2(R_{1x} + K_{1x})}, \quad a_5 = \frac{K_{3x}}{3(R_{1x} + K_{1x})}. \tag{14}$$

Thus, if nonlinear processes occur with zero rates ($R_{2x} = K_{2x} = K_{3x} = 0$), the relative yield will be perfectly proportional and obtained as $Y_R = 1$. The relative yields calculated from Eq. (13) for BaF_2 and BGO:Ce are shown in Fig. 1, which shows that the nonproportionality in GSO occurs over a wider energy range, 10–10^5 keV, in comparison with 10–100 keV in BaF_2.

Although BaF_2 is an intrinsic and GSO:Ce is a doped (extrinsic) scintillator, it is interesting to note that their light yield dependence (Fig. 1) on energy suggests that both are excitonic scintillators. In BaF_2, the formation of excitons can be understood, but in GSO:Ce the scintillation mechanism represents the immediate capture of holes at Ce^{3+} and raises the question whether exciton formation takes place before the capture of holes. In most inorganic semiconductors, the formation of excitons occurs within nanoseconds (dielectric constant $\varepsilon \geq 10$), but in organic solids ($\varepsilon \approx 3$), the formation of excitons occurs much faster, at the instant e-h are excited because the binding energy between the excited e and h is about four times larger than in silicon ($\varepsilon = 12$). The dielectric constant of BaF_2 ($\varepsilon \approx 2.25$) and GSO:Ce ($\varepsilon \approx 3.4$)[26] compares with that of organic solids and, hence, the exciton formation has to be very fast, and it may occur prior to the capture of holes. However, the magnitude of the dielectric constant may not be the only factor responsible for this mechanism, because most known inorganic scintillators have a dielectric constant lower than that of silicon.

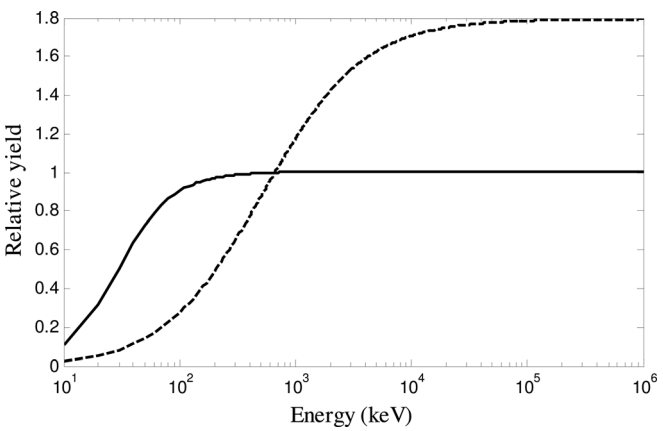

FIG. 1. Calculated relative light yield from Eq. (13) for two excitonic scintillators. GSO: dashed curve and BaF_2: solid line curve.

B. Non-excitonic scintillators

This represents the class of scintillating materials in which the excited e-h pairs remain unbound and do not form excitons. The light yield in these materials shows a hump in the mid-energy range, as observed in most alkali halides and CaF_2:Eu.[6] This is discussed further in the Sec. IV. In this case, $f_x \sim 0$, $a_2 \neq 0$, and $a_3 = 1$, which give the relative yield from Eq. (11) as

$$Y_R = \frac{(a_1 + a_2 Q E^{-1})(1 + a_4 Q(662\,\text{keV})^{-1} + a_5 Q^2 (662\,\text{keV})^{-2})}{(a_1 + a_2 Q(662\,\text{keV})^{-1})(1 + a_4 Q E^{-1} + a_5 Q^2 E^{-2})}, \tag{15}$$

where the rate coefficients a_1, a_2, a_4, and a_5 are different from those in Eq. (13) and are given by

$$a_1 = \frac{R_{1eh}}{R_{1eh} + K_{1eh}}, \quad a_2 = \frac{R_{2eh}}{2(R_{1eh} + K_{1eh})},$$
$$a_4 = \frac{(R_{2eh} + K_{2eh})}{2(R_{1eh} + K_{1eh})}, \quad a_5 = \frac{K_{3eh}}{3(R_{1eh} + K_{1eh})}. \tag{16}$$

According to the rates given in Table II, $R_{1eh} = 0$, which makes $a_1 = 0$ from Eq. (16) for all the four scintillators and then the relative yield in Eq. (15) becomes independent of a_2, provided it is not zero. The relative light yield calculated using Eq. (15) for NaI:Tl is shown in Fig. 2 (solid line). As far as the proportionality in the relative light yield is concerned for this category of scintillators, these are the most difficult ones to make them proportional, particularly if $R_{1eh} = 0$. In this case, even if the nonlinear processes have zero rates ($R_{2eh} = K_{2eh} = K_{3eh} = 0$), Y_R (Eq. (15)) will still be inversely proportional to E. This is an interesting case because the linear radiative rate is zero, which means that the nonlinear rates are dominant over the linear rates and, therefore, such a scintillator cannot be made proportional.

C. Intermediate scintillators

This is the case when $0 < f_x < 1$ and the excitations created within the track consists of both excitons and e-h pairs. This may be considered to be the most common category, and the above two cases are the limiting special cases of this category. Most scintillators, like NaI:Tl, CsI:Tl, $LaCl_3$, etc., may be classified in this category, and the relative yield can be calculated from Eq. (11). For NaI:Tl, the calculated relative yields at four different values of $fx = 0.0$, 0.1, 0.5, and 1.0 are shown in Fig. 2. The relative yield in $LaCl_3$ is shown in Fig. 3 for $f_x = 0.0$, 0.1, 0.6, and 1.0. This parameter f_x appears to play a very significant role in the nonproportionality. For $f_x < 0.5$ and rates given in Table I, although the yields in BaF_2 and GSO at varying f_x are not shown here, all the four scintillators show a higher order of non-proportionality in the whole energy range (see Figs. 2 and 3).

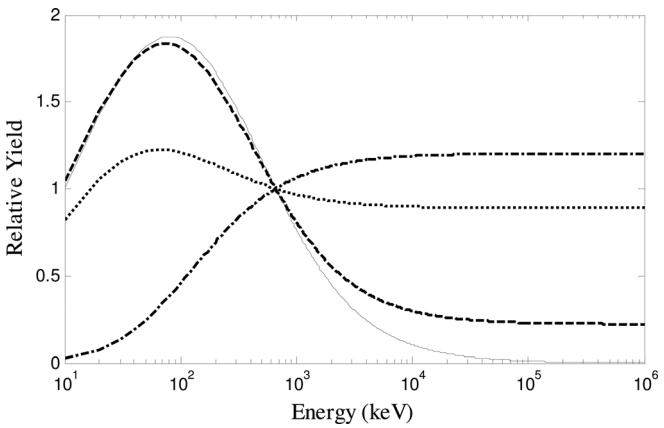

FIG. 2. Relative yield in NaI:Tl as a function of the incident energy and the fractional excitonic concentration f_x. Solid line curve $f_x = 0.0$ (non excitonic) (Eq. (15), dashed curve $f_x = 0.1$, dotted curve $f_x = 0.5$ (Eq. (11)) and dashed-dotted curve $f_x = 1.0$ (pure excitonic) (Eq. (13)).

IV. DISCUSSION

Following a phenomenological approach, the relative scintillator yield is derived and calculated for four scintillators, namely NaI:Tl, BaF_2, GSO, and $LaCl_3$. The relative yields shown in Figs. 1–3 are found to be nonproportional. In some cases, the yield is nonproportional only in the lower energy range, 10-100 keV. The shapes of the calculated relative yields agree qualitatively but reasonably well with those observed[27] in all the four scintillators considered here.

Considering only two channels, one radiative and one non-radiative, Jaffe[5] has fitted the experimental scintillator yield data for seven scintillators to the relative yield in the form of

$$Y'_R = \frac{(662\text{keV})^{-\alpha} + K^{-\alpha}}{E^{-\alpha} + K^{-\alpha}}, \tag{17}$$

where α and K are the parameters determined by this fitting. In order to get an insight of the yield in Eq. (17), the author has recently[28] derived the relative yield in the form of Eq. (17) by considering $a_2 = a_5 = 0$ in Eq. (7). This derivation reveals analytical values of the fitting parameters as $\alpha = 1$ and $K = \frac{a_4}{a_3} Q$ and as $a_3 = 1$, $K = a_4 Q$. According to Eq. (6), the assumption of $a_5 = 0$ means the neglect of Auger processes of non-radiative recombination, and $a_2 = 0$ is satisfied by the excitonic scintillators ($f_x = 1$) with $R_{2x} = 0$. In this case, there are two scintillators, BaF_2 and GSO, considered

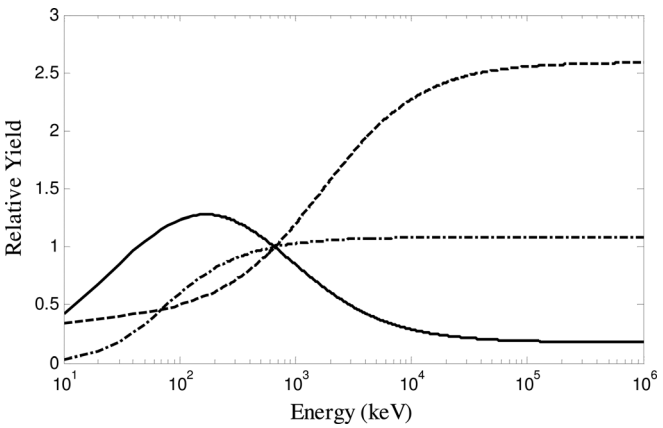

FIG. 3. Relative light yield of $CaCl_3$:Ce as a function of the incident energy and fractional excitonic concentration fx. Solid line for $fx = 0.1$, dashed line for $fx = 0.6$, and dashed-dotted line for $fx = 1.0$ (pure excitonic).

here for which, according to Eq. (14), $a_4 = K_{2x}/(2(R_{1x} + K_{1x}))$. If the rate of Auger recombination K_3 is neglected, then using the rates in Table II, we get $\alpha = 1$ for both and $K = 3$; 44 keV for BaF_2 and 521.16 keV for GSO. These two scintillators have also been considered in Ref. 5, and by fitting Eq. (17) to the experimental data, the two parameters are obtained as $\alpha = 1.44$ and K = 4.28 keV for BaF_2 and $\alpha = 0.87$ and K = 2.98 keV for GSO. While the values of α calculated here agree quite well with those obtained by Jaffe[5] for both BaF_2 and GSO, the value of K agrees only for BaF_2, but for GSO, the calculated value is more than two orders of magnitude larger than that obtained by Jaffe. This discrepancy between BaF_2 and GSO is also reflected in the light yield of the two scintillators plotted in Fig. 1, although both are apparently excitonic scintillators. The discrepancy can be attributed only to the differences in the values of rates and radius of the track. According to Table II, the sum of the linear rates of radiative and nonradiative recombinations for GSO are about two orders of magnitude lower than those for BaF_2, and the other difference is the track radius for GSO is considered twice of that for BaF_2. All other rates are assumed to be identical for both the scintillators. It is important to realize that the parameter K depends on both the linear rates and track radius because Q depends on the track radius (see above). The sum of linear rates appears in the denominator of K and, hence, enhances its value by two orders of magnitude for GSO. Also, Q in Eq. (8) is inversely proportional to the square of the track radius, so this should lower down the value of Q by a factor of four in comparison with that for BaF_2. As a result, the value of K for GSO becomes two orders of magnitude higher. This provides further insight on the nonproportionality in the relative yield of BaF_2 and GSO that, if the radiative excitonic lifetime ($\tau_x^{-1} = R_{1x} + K_{1x}$) is short, then the nonproportionality may occur only in the lower energy range, 10–100 keV. A prolonged radiative excitonic lifetime causes nonproportionality to stretch to higher energy range (see, for example, GSO in Fig. 1). Apparently, experimentally, the light yield presented for GSO and BaF_2 in Ref. 5 are quite similar; not as different as shown in Fig. 1 here, revealing that the linear rates in BGO and BaF_2 may not be as different as used here. This implies that the sum of linear rates ($R_{1x} + K_{1x}$) for GSO has been drastically underestimated here because a difference of two orders of magnitude in comparison with BaF_2 is very significant. This is, unfortunately, a problem in most scintillators that rates of excitation processes are not very well studied.

Not only the rates of excitation processes, but also the effect of excitation distribution, f_x, within the track need to be studied very closely for understanding the nonproportionality. In Fig. 2, the relative light yield in NaI:Tl is plotted as a function of the incident energy for four different values of $f_x = 0.0$, 0.1, 0.5, and 1.0, keeping the same values of all the rates. It is quite obvious that, as f_x increases, the nonproportionality which is spread in the full energy range for $f_x = 0.0$ starts reducing and eventually remains only in the lower energy range, 10-1000 keV, $f_x = 1$, and becomes proportional in the higher energy range. This implies that, for reducing the nonproportionality in scintillators, the fractional excitonic population within the track should be dominantly high in comparison with the e-h pair population. This situation may very well depend on the rates of all processes; however, the strength of binding energy for the formation of an exciton depends inversely on the static dielectric constant of the material and separation between the excited e-h pair. This suggests that scintillators of low dielectric constant material may be found to be relatively more proportional than those with high dielectric constant because the probability of creating excitons in the former will be higher. However, this is not a well established observation in inorganic scintillators. It is well known that organic materials have lower dielectric constant ~ 3 in comparison with inorganic scintillator materials $\sim$ 5-9, and excited e-h pairs form excitons easily in organics. The low dielectric constant of organic scintillators increases the rate of radiative recombination (shorter decay time) which is established,[29] one of the reasons organic materials are better suited for fabricating organic light emitting devices than organic solar cells.

The fourth scintillator studied here is $CaCl_3$:Ce, for which the calculated relative yield is shown in Fig. 3 as a function of the incident energy for three values of $f_x = 0.1$, 0.6, and 1.0. This is a relatively new scintillator discovered nearly a decade ago,[30,31] and together with $LaBr_3$:Ce, two are known to have better proportionality and considered to be among the best scintillators known for x ray and for gamma ray detection.[32,33] Khodyuk and Dorenbos[4] have recently studied the nonproportional response of these two scintillators in the low energy range 9-100 keV experimentally using highly monochromatic synchrotron irradiation. They have studied two types of nonproportionalities: nonproportionality with respect to photon energy, called photon-nonproportionality, and that with respect to electron energy called electron-nonproportionality. From this definition, in this paper, we have studied the photon nonproportionality theoretically. The light yield plotted in Fig. 3 for $f_x = 1$ in the energy range 10–100 keV agrees qualitatively with its shape, measured experimentally in Ref. 4. The main difference is the dips that have been observed corresponding to energies of K_α-escape and K_β-escape, which do not show up in Fig. 3 (dashed-dotted curve) due to the phenomenological approach followed here. No mechanism for accounting the K_α-escape and K_β-escape energies has been introduced in this approach. This qualitative agreement with the experimental results does indicate that $LaCl_3$:Ce may be operating dominantly as an excitonic scintillator. Also $LaBr_3$:Ce has similar characteristics.[4] According to the relative yield in Eq. (13), $LaCl_3$:Ce can be made perfectly proportional if the bimolecular and Auger processes are eliminated from occurring (i.e., $a_4 = a_5 = 0$) within the track.

A. Reduction of nonproportionality

According to the analysis of the relative light yield presented here, one may consider reducing nonproportionality through the following approaches: 1) under the high excitation density condition, the track should contain dominantly more excitons than e-h pairs, which essentially means that the linear rate of radiative recombination must be quite high,

2) depletion of the high excitation density condition from the track at a faster rate than the rate of activation of bimolecular and Auger processes, and 3) creation of large carrier concentration gradient of carriers/excitations to promote faster radial diffusion of electrons and holes from the track. Attempts of achieving any one or more of the three conditions in a scintillator are challenging, but if successful, will deplete the excitation concentration from the track non-destructively and reduce the probability of occurrence of nonlinear processes.

The linear radiative recombination of excitons and excited e-h pairs occurs in a time range of nano to micro seconds (10^{-10}–10^{-7} s), and linear nonradiative recombination occurs at an order of magnitude longer time scale for the four scintillators (see Table II) considered here. The nonlinear nonradiative (quenching) and diffusion processes compete with each other at a similar time scale of picoseconds or shorter.[9] On one hand, this is not good news for proportionality if nonlinear quenching occurs faster than the radiative recombination. On the other hand, if the mobility of carriers is large enough to help carriers diffuse away from the track efficiently, the high density situation will be relieved, which will reduce/eliminate the occurrence of non-linear quenching prior to radiative recombination. Through simulation, Williams *et al.*[9] have recently studied the effect of magnitude of mobility of charge carriers and that of the difference between the electron and hole mobilities on the carrier diffusion profile in CsI: Tl (0.3%) (cesium iodide doped thallium). In this modeling, they have considered the electron mobility $\mu_e = 8\text{cm}^2/\text{Vs}$, hole mobility $\mu_h = 0$ (Table I), and dielectric constant of 5.65. For two different excited e-h concentrations of 2.5×10^{18} and 2.5×10^{20} e-h cm^{-3}, two different times of reaching steady-state $t_{SS} = 9.5$ ps and 0.4 ps, respectively, are obtained. During this ~ 10 ps, the excited e-h density along the cylindrical track axis reduces by about one order of magnitude when the exciting e-h density is 2.5×10^{20} e-h/cm^3 but does not change much in the case of low excitation density 2.5×10^{18} e-h cm^{-3}. They have also determined the time dependent bimolecular quenching rate $K_2 = 2.4 \times 10^{-15} t^{-1/2}$ cm^3/s and radiative lifetime $\tau_r = 1.4$ ns. Evaluating K_2 at t_{SS}, we get $K_2 = 7.7 \times 10^{-10}$ cm^3/s and 3.8×10^{-9} cm^3/s for the excitation densities 2.5×10^{18}cm^{-3} and 2.5×10^{20} cm^{-3}, respectively, and $K_2 = 6.4 \times 10^{-11}$ cm^3/s at $\tau_r = 1.4$ ns. The bimolecular rate, K_2, chosen here (Table II) for exciton and e-h pairs for all the four scintillators are 3×10^{-12} cm^3/s and 2×10^{-11} cm^3/s. These rates are closer to those calculated in Ref. 9 at $\tau_r = 1.4$ ns.

The track radius considered here for the four scintillators varies from 2 nm to 6 nm. Considering the example of CsI:Tl,[9] the exciton density reduces to a little more than half at the radial distance of 2 nm at the initial time to more than one order of magnitude at $t_{SS} = 9.5$ ps for the excitation density of 2.5×10^{18} e-h cm^{-3}. For the excitation density of 2.5×10^{20} e-h cm^{-3}, the reduction in the excitation density is just more than half at both times. At a radial distance of 4 nm, the axial excitation densities reduce by more than 20 times, and at 6 nm, the reduction is by 2 orders of magnitude for both the excitation densities. Although the track radii of 2 nm, 4 nm, and 6 nm are not used in the calculation here for the same scintillator, this reduction analysis is compared for only one scintillator CsI:Tl in.[9] This is an interesting result, because even if the bimolecular quenching rate is non-zero depending on the carrier mobility, if the diffusion process is fast enough to relieve the high excitation density situation from the track, the bimolecular quenching process will not be effective and will not contribute to nonproportionality. As it has been pointed out in Ref. 9, the bimolecular quenching process also reduces the high excitation density, but this reduction occurs by reducing the original excitation density and, hence, contributes to the nonproportionality. In contrary to this, the reduction of high density in the track by diffusion does not kill the initial excitation density and, hence, contributes only to the proportionality.

B. Track length

It is also desirable to discuss the significance of the track length derived in Eq. (4) under the approximation of average track radius, in which case, the track length is obtained independent of the track radius, but it is proportional to the square of the initial incident energy. Under this approximation, an incident γ-photon of energy 10 keV will have a track length of two orders of magnitude less than that of a 100 keV photon. However, according to Eq. (3), a 10 keV photon will create 10 times more excitations than a 100 keV photon. Thus, for the same track radius in a cylindrical volume $V = \pi r^2 L$, a 10 keV photon will have three orders of magnitude higher excitation density than a 100 keV photon. This obviously reveals the fact that the excitation densities at lower energies are too high to reduce to a point where the bimolecular process can be eliminated and, hence, the nonproportionality occurs more so in the lower energy range than higher energy range. This analysis obviously supports the results presented here that all scintillators are nonproportional in the lower energy range 10 keV to 100 keV and also agrees with the experimental results.[2,4,27,30,31] In semiconductors, e.g., Ge, according to Table I, in comparison with CsI:Tl, the carrier mobilities are more than two orders of magnitude higher, leading to faster diffusion from the track, avoiding completely the occurrence of bimolecular or higher nonlinear processes.[8] Therefore, the light yield in Ge is proportional in all energy ranges, including the lower one.

It may be desirable to include a discussion about the light yield in the lower energy range < 10 keV, which can be easily calculated from Eq. (7) but not presented here. This is important, because the largest energy loss $(-dE/dx)$ is found experimentally to occur at the final stages of energy dissipation in the primary electron track. According to Eq. (1), at largest $(-dE/dx)$, the excitation density $n(x)$ will be the highest, and this occurs when the incident energy E reduces to the order of 100 eV (see Eq. (3)). The highest excitation density implies smallest inter-excitation separation and, therefore, the nonlinear processes can be expected to be very effective, as discussed above, and, hence, the light yield will be highly nonproportional in this energy region. The light yield of all scintillators considered here and calculated from Eq. (7), as plotted in Figs. 1–3, continues decreasing in the energy range 0-10 KeV. However, if we could really find

new materials or modify the existing ones to have high carrier mobilities so that the excitations (e-h) can diffuse away faster from the track before they decay through the nonlinear processes, then the proportionality can be achieved in this energy range as well.

V. CONCLUSION

The nonproportionality of four inorganic scintillators is studied by calculating the scintillator light yield as a function of the rates of radiative and nonradiative linear and nonlinear processes, including bimolecular and Auger. The light yield thus calculated agrees qualitatively with the experimental results for scintillators considered here. It is found that, if the nonlinear quenching processes can be prevented from occurring in a scintillator, the nonproportionality can be eliminated. However, the nonlinear quenching processes are inevitable from occurring under the high excitation density condition unless some mechanism, like diffusion, can compete with the nonlinear quenching. The diffusion rate depends on the mobility of charge carriers and, therefore, materials with higher charge carrier mobility are expected to be more proportional. However, mobility measurements for scintillators are unfortunately scarce in the literature. Measuring mobility and inventing scintillating materials with higher charge carrier mobility may bring a new variety of inorganic proportional scintillators.

ACKNOWLEDGMENTS

The author is grateful to Professor Richard Williams, Wake Forest University, Winston Salem and Dr. Bill Moses, Lawrence Berkeley National Laboratory, Berkeley, USA for several discussions during the course of this work.

[1]P. J. Roach and D. L. Baily, Intern. Med. J. **35**, 577 (2005).
[2]P. Dorenbos, J. T. M. de Haas, and C. W. E. van Eijk, IEEE Trans. Nucl. Sci. **NS-42**, 2190 (1995).
[3]M. Moszynski, J. Zalipska, M. Balcerzyk, M. Kapusta, W. Mengesha, and J. D. Valentine, Nucl. Instrum. Methods A **484**, 259 (2002).
[4]I. V. Khodyuk and P. Dorenbos, J. Phys.: Condens. Matter **22**, 485402 (2010).
[5]J. E. Jaffe, Nucl. Instrum. Methods Phys. Res. A **580**, 1378 (2007).
[6]G. E. Bizarri, W. W. Moses, J. Singh, A. N. Vasile'v, and R. T. Williams, J. Appl. Phys. **105**, 044507 (2009).
[7]J. E. Jaffe, D. V. Jordan, and A. J. Peurrung, Nucl. Instrum. Methods Phys. Res. A **570**, 72 (2007).
[8]Q. Li, J. Q. Grim, R. T. Williams, G. A. Bizarri, and W. W. Moses, "The role of hole mobility in scintillator proportionality," Nucl. Instrum. Methods Phys. Res. A (to be published).
[9]R. T. Williams, J. Q. Grim, Q. Li, K. B. Ulcer, and W.W. Moses, Phys. Status Solidi B **248**, 426 (2011).
[10]B. P. Aduev, E. D. Aluker, G. M. Belokurov, and V. N. Shvayko, Phys. Status Solidi B **208**, 137 (1998).
[11]S. S. Li and W. R. Thurker, Solid-State Electron. **20**, 609 (1977).
[12]J. M. Dorek and Ph. Leturcq, Solid-State Electron. **24**, 821 (1981).
[13]C. F. Jacoboni, F. Nava, C. Canali, and G. Ottaviani, Phys. Rev. B **24**, 1014 (1981).
[14]O. A. Gilkova, B. Ya. Moizhez, and L. S. Stilbans, Sov. Phys. Solid State **3**, 2259 (1962).
[15]J. C. Erickson, H. W. Yao, R. B. James, H. Herman, and M. Greaves, J. Electron. Mater. **29**, 699 (2000).
[16]Z. He and R. D. Vigil, Nucl. Instrum. Methods Phys. Res. A **492**, 387 (2002).
[17]H. L. Malm, IEEE Trans. Nucl. Sci. **19**, 263 (1972).
[18]R. Minder, G. Ottaviani, and C. Canali, J. Phys. Chem. Solids **37**, 417 (1976).
[19]Wm. C. McHarris, Nucl. Instrum. Methods Phys. Res. A **242**, 373 (1986).
[20]G. M. Haarberg and J. M. Egan, Ber. Bunsenges. Phys. Chem. **102**, 1298 (1998).
[21]S. Kubota, F. Shirraishi, and Y. Takami, J. Phys. Soc. Jpn. **69**, 3435 (2000).
[22]R. K. Ahrenkiel and F. C. Brown, Phys. Rev. **136**, A223 (1964).
[23]W. Setyawan, R. M. Gaume, R. S. Feigelson, and S. Curtarolo, IEEE Trans. Nucl. Sci. **56**, 2989 (2009).
[24]J. Singh and K. Shimakawa, *Advances in Amorphous Semiconductors* (Taylor & Francis, London, 2003).
[25]H. A. Bethe, Ann. Phys. **5**, 325 (1930).
[26]W.-M. Yao *et al.*, J. Phys. G **33**, 1 (2006).
[27]W. Mengesha, T. Taulbee, B. Rooney, and J. Vlentine, IEEE Trans. Nucl. Sci. **45**, 456 (1998).
[28]J. Singh, J. Phys.: Conf. Ser. **253**, 012016 (2010).
[29]G. Laustrat, "The luminescence decay of organic scintillators," in *Organic Scintillators*: *Proceedings of the International Symposium on Organic Scintillators*, edited by D. L. Horrocks (Gordon and Breach, New York, 1966).
[30]J. Andriessen, O. T. Antonyak, P. Dorenbos, P. A. Rodnyi, G. B. Stryganyuk, C. W. E. van Eijk, and A. S. Voloshinovskii, Opt. Commun. **178**, 355 (2000).
[31]E. V. D. van Loef, P. Dorenbos, C. W. E. van Eijk, K. Kraemer, and H. U. Guedel, Appl. Phys. Lett. **77**, 1467 (2000).
[32]A. Iltis, M. R. Mayhugh, P. Menge, C. M. Rozsa, O. Selles, and V. Solovyev, Nucl. Instrum. Methods A **563**, 359 (2006).
[33]W. W. Moses and K. S. Shah, Nucl. Instrum. Methods A **537**, 317 (2005).